

THE INFLUENCE OF CLIMATE CHANGE ON THE WATER QUALITY OF STAGNANT, ICE-COVERED, EUTROPHIC WATER BODIES

Kouki SUGIHARA¹ and Makoto NAKATSUGAWA²

¹Member of JSCE, Civil Engineering Research Institute for Cold Region, Public Works Research Institute
(Hiragishi 1-3-1-34, Toyohira-ku, Sapporo 062-8602, Japan)

E-mail: sugihara-k@ceri.go.jp

²Member of JSCE, Professor, College of Environmental Technology, Muroran Institute of Technology
(Mizumoto-tyo 27-1, Muroran 050-8585, Japan)

E-mail: mnakatsu@mmm.muroran-it.ac.jp

This study clarifies the water quality characteristics of stagnant, eutrophic water bodies that freeze in winter, based on our surveys and simulations, and examines how climate change may influence those characteristics. The survey found that climate-change-related increases in water temperature were suppressed by ice covering the water area, which also blocked oxygen supply. It was also clarified that the bottom sediment consumed oxygen and turned the water layers anaerobic beginning from the bottom layer, and that nutrient salts eluted from the bottom sediment. The eluted nutrient salts were stored in the water body until the ice melted. Climate change was surveyed as having caused decreases in nutrient salts concentration because of the shortened ice-covered period; however, Biochemical Oxygen Demand (BOD) showed a tendency to increase because of the proliferation of phytoplankton that was promoted by the climate-change-related increase in water temperature in spring.

To forecast the water quality by using these findings, particularly the influence of climate change, we constructed a water quality simulation model that incorporated the freezing-over of water bodies. The constructed model showed good temporal and spatial reproducibility and enabled water quality to be forecast throughout the year, including during the ice-covered period. The forecasts using the model agreed well with the survey results of the shortened ice period and climate-change-related increase in the BOD in spring.

Key Words : *eutrophication, freezing, ecosystem model, climate change*

1. INTRODUCTION

The adverse effects of climate change on water bodies are expected to result in the reduction of global water resources and the deterioration of water quality¹⁾. Based on a statistical analysis of water quality data for Lake Kasumigaura and public water bodies, Fukushima et al.^{2), 3)} reported that increases in primary production in waters due to global warming had resulted in water quality deterioration. Mori⁴⁾ compared the water quality of the Kiso River between years of relatively high temperatures and years of average temperatures, and concluded that global warming had increased the BOD in the river by accelerating the development of an anoxic condition in the river during summer. In addition to these studies, several studies^{5), 6), 7)} have addressed processes leading to water quality problems in stagnant water areas,

measures against these problems, and the like. Many of these water quality problems are induced by oxygen-free conditions. Specifically, thermal stratification, which intensifies during summer due to an anoxic condition, inhibits the vertical circulation of water masses in water areas. Anoxic conditions in summer have been reported nationwide, and a wealth of observation data is available.

On the other hand, observation data are insufficient regarding water quality in winter, particularly the quality of water in areas that freeze in winter; thus, little is known about variations in water quality in winter. The reasons for the lack of observation data include the difficulty of observation due to river freezing and the fact that significant water quality problems do not occur in winter. In cold, snowy regions, such as Hokkaido, it is not unusual for stagnant water areas to freeze over for the roughly five

months from December through April. Regarding eutrophic lakes, in which vertical mixing takes place in spring and autumn, it is very important to understand when the lakes freeze over and how the lake water quality varies during the freezing season, in order to analyze the temporal changes in water quality. In Lake Harutori⁸⁾, a brackish lake in eastern Hokkaido, immersion instruments were used for observing the vertical distributions of water temperature, dissolved oxygen (DO) and electric conductivity during the freezing season. The observation results showed that a wedge of saltwater suppresses the vertical mixing of water and that, thus, an anoxic condition develops in the lake. In Lake Abashiri⁹⁾, another brackish lake in eastern Hokkaido, water sampling was conducted, in addition to observation by immersion-type instruments, in order to analyze the vertical distribution of nutrient salts. The concentration of nutrient salts was reported to be higher in the bottom water layer than in the water layers above it. Ohtaka et al.¹⁰⁾ conducted water sampling and observation by means of immersion-type instruments in a freshwater lake and reported that an anoxic condition developed and ammonium nitrogen increased while the lake was frozen over. Vertical observation of water quality in frozen rivers/lakes was conducted in some studies¹¹⁾⁻¹³⁾ overseas, but these focused on dissolved oxygen and plankton composition rather than on temporal variations in the concentration of nutrient salts. Although the results of all these studies indicate that an anoxic condition develops and nutrient salts increase in frozen rivers/lakes, causal relationships between water freezing and temporal changes in the concentration of nutrient salts have not been quantitatively evaluated.

Based on river and lake freezing and breakup records worldwide, the IPCC Fourth Assessment Report¹⁾ states that the freezing date has become later by 5.8 ± 1.6 days per century and the breakup date has become earlier by 6.5 ± 1.2 days per century. It is reported that the duration of ice cover has decreased due to the increase in annual mean air temperature. However, little is known about how the shorter duration of ice cover affects the water quality.

It is presumed that a reduction in the duration of ice cover due to the increase in mean air temperature results in a shortening of the period during which an anoxic condition develops in water. The result would be less water quality deterioration than in the case of a longer duration of ice cover. However, it is also possible that water quality would deteriorate due to the temperature increase following the breakup of river and lake ice. The consequences of these factors in combination have not been elucidated. In view of this, a study was conducted to understand how the water quality of a frozen river varied and how a re-

duction in the duration of ice cover due to climate change affected the river water quality.

The content of the study is outlined below. Data used in this study are from firsthand observations of rivers as well as from laboratory tests conducted by the Sapporo Development and Construction Department of the Hokkaido Regional Development Bureau.

(a) Analyze the results of water quality surveys of a frozen river, as well as the results of laboratory experiments conducted by using bottom sediment, for the purpose of understanding variations in water quality in the frozen river.

(b) Collate existing water quality survey results and meteorological data in order to analyze how the water quality varies and how the increase in mean air temperature affects river freezing.

(c) Develop a material cycle model that takes river freezing into account for the purpose of facilitating full-year water quality predictions.

2. RIVER FOR OBSERVATION

Data analyzed in this study are on the Barato River (**Fig.1**), which flows through the northern part of Sapporo. The Barato River is part of the Ishikari River. It was cut off when the Oyafuru Shortcut was excavated for flood control in 1931. The Barato River is 20km long and has an average width of 200m and an average depth of 2.3m. The deepest part of the river is 15m deep. One of the hydrological characteristics of the Barato River is the disturbance of flow at two narrowed sections (Yamaguchi Bridge and Kannon Bridge). Additionally, because the lower course of the Barato River connects to the Ishikari River via the Shibi Canal, the Barato River is a backwater of the Ishikari River and is strongly influenced by tides in Ishikari Bay. Thus, the Barato River is a semi-closed water area where the river water retention time ranges from 8 to 20 days¹⁴⁾. Pollution load, or effluent from the city of Sapporo, enters the river via the Sosei River and the Fushiko River, and algal blooms have been observed in the Barato River. When the river freezes over in winter (**Photo 1**), people visit to enjoy ice fishing for smelt.

The water area upstream of the Yamaguchi Bridge (i.e., a river section including the upper lake basin shown in **Fig.1**) connects to the lower course via a 10m-wide channel under the Yamaguchi Bridge. A hydrological feature¹⁴⁾ of this water area is that the river current flows alternately downstream (from the upper lake basin toward Kannon Bridge) and upstream (from Kannon Bridge toward the upper lake basin) at rate of $0\text{--}5\text{m}^3/\text{s}$. The stagnation of the water in this river section is the most significant of any stagnation in the Barato River. Pollutant load is

supplied by backflow, the internal production of organic matter and the disturbance of bottom sediment¹⁵⁾. To improve the river water quality, water has been channeled from the Ishikari River into the Barato River at its upstream edge since June 2010. However, it is not possible to bring in water from the Ishikari River when it freezes in winter. Thus, an understanding of the variations in river water quality during the freezing period is also necessary for evaluating how water from the Ishikari River has helped improve the water quality of the Barato River.

3. OBSERVATION METHOD

Regarding the St.A shown in **Fig.1**, the Hokkaido Regional Development Bureau¹⁶⁾ has been conducting bottom sediment analysis, stationary measurement and vertical observation by means of self-recording instruments, water sample analysis and elution tests of undisturbed bottom sediment core samples from the upper lake basin. The methods used are explained below.

(a) Bottom sediment analyses: On October 5, 2009, bottom sediment samples were collected at St.A by using an Ekman-Birge bottom sampler for the purpose of analyzing bottom sediment for chemical oxygen demand (COD), total nitrogen (T-N), total phosphorus (T-P), ignition loss, sulfide, and density and median diameter of sediment particles.

(b) Stationary observation by means of self-recording instruments: **Fig.2** shows a cross-section of St.A. The self-recording instrument IOTechnic HJ-402 (the black circle in **Fig.2**) was set at 1m above the bottom sediment in the center of flow in St.A, and the water temperature and the DO level were continuously measured at one-hour intervals from October 8, 2009 through March 15, 2010.

(c) Instrumental vertical observation and water quality analysis: A Van Dorn water sampler was used for collecting water samples at the depths of 0.5m, 3m, and 5m from the ordinary water level (indicated by white circles in **Fig.2**), and the water quality of the samples was analyzed. The water samples were analyzed for BOD, COD [Mn], T-P, orthophosphate ($\text{PO}_4\text{-P}$), T-N, nitrite nitrogen ($\text{NO}_2\text{-N}$), nitrate nitrogen ($\text{NO}_3\text{-N}$), ammonium nitrogen ($\text{NH}_4\text{-N}$) and chlorophyll a (Chl-a).

A general dilution method (JIS K 0102 (2008)-21, 32.1) was employed for the analysis of BOD. In this method, high DO is indicative of oxygen production by phytoplankton. But when measured blank values are subtracted from the values of DO of inoculated samples, these samples have low DO levels and contain little oxygen produced by plankton. In this study, BOD is regarded as an indicator of the amount of substances, and the amount of substances corre-

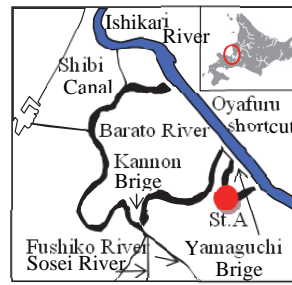


Fig.1 View of the Barato river.



Photo 1 Freeze beginning at St.A in December.

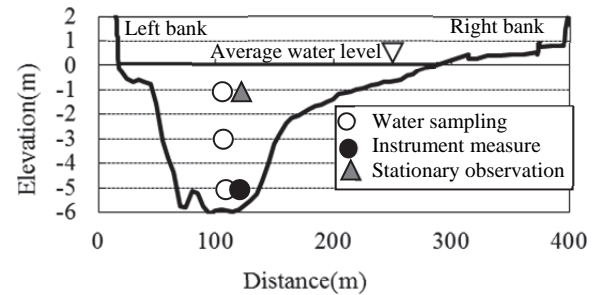


Fig.2 Cross section of St.A.



Photo 2 View of observation when thin ice formed.



Photo 3 View of observation on ice.

lates with the quantity of phytoplankton and organic matter. In other words, it is assumed that a DO level that includes the oxygen produced by phytoplankton indicates the amount of substances that can be correlated with the quantity of organic matter supplied by phytoplankton and inflow of water.

To observe the vertical distributions of water temperature, turbidity and DO level, measurements were taken at intervals of 0.5m by using immersion instruments (i.e., ACL208-PDK [Alec Electronics Co., Ltd.] and YSI6600 [YSI Nanotech Japan]). Measurements were taken seven times: on December 7 in 2009, on January 12, 19, and 27 in 2010 and on February 8, 15, and 22 in 2010. Because the ice cover in December was too thin for researchers to stand on, a boat was used for breaking ice and taking measurements (**Photo 2**). In January and February, a borehole was used for observation (**Photo 3**).

(d) Elution test: A diver collected undisturbed bottom sediment samples from St.A. Elution tests were conducted by filling acrylic tubes with water that had been collected from the upper lake basin on October 5, 2009. The water from the upper lake basin was also used for a controlled test in which the water

was not exposed to bottom sediment. Because water temperatures near bottom sediment during the freezing period of the river were not known, sediment samples were analyzed at a laboratory temperature of 15°C to simulate the temperature of the bottom-layer water on October 5, 2009 when the bottom sediment samples were collected. The analysis continued for 30 days under anoxic conditions. The testing device is outlined in **Fig.3**, and the test setup is shown in **Photo 4**. Sediment samples were analyzed for BOD, COD, T-P, T-N, PO₄-P, NO₂-N, NO₃-N, and NH₄-N.

The measurement and testing explained above were conducted by the Sapporo Development and Construction Department of the Hokkaido Regional Development Bureau. Data provided to this study were analyzed as described below.

4. OBSERVATION RESULTS

(1) Bottom sediment analysis results

The bottom sediment analysis results are summarized in **Table 1**. Analysis results concerning bottom sediment samples collected near the Shibi Canal (**Fig.1**) are also shown for comparison. The Shibi Canal is strongly influenced by backflow from the Ishikari River; thus, the water quality of this canal is similar to that of the Ishikari River. In **Table 1**, the COD and ignition loss are much greater in the upper lake basin than in the Shibi Canal, suggesting that the bottom sediment in the upper lake basin is high in organic matter. This seems to be why the values of density and median diameter of sediment particles are relatively small in the upper lake basin. Additionally, the sediments in the upper lake basin are likely to be eutrophic, as they have a high content of nitrogen and phosphorus.

(2) Results of instrument observations

a) Results of stationary measurement by means of self-recording instruments

Figure 4 shows the results of stationary measurement by means of self-recording instruments. Measured DO saturation values and water temperatures were used for calculating DO. Air temperature data from the nearby station of the Automated Meteorological Data Acquisition System (AMeDAS) in Ishikari are also shown for reference.

On December 16 when the air temperature dropped below zero, the water temperature began to increase and the DO level began to plunge (See **Fig.4**). The DO level kept decreasing, and reached zero on January 30. It remained at zero until the end of the measurement period. Diurnal variation in water temperature and DO was great when the water temperature was 5°C or higher (from October 8

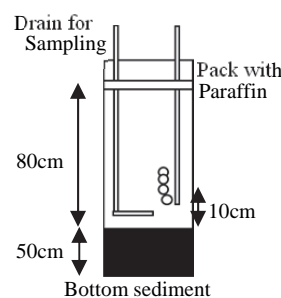


Fig.3 Schematic figure of test device.



Photo 4 Overview of test device.

Table 1 Result of sediment analysis.

Analysis	unit	St. A	Shibi canal
COD	mg/g	38.9	13.6
T-N	mg/g	5.00	1.32
T-P	mg/g	2.07	1.20
Ignition Loss	%	11.60	4.86
Sulfide	mg/g	1.76	0.22
Density	g/cm ³	2.402	2.614
Median Diameter (D50)	mm	0.009	0.399

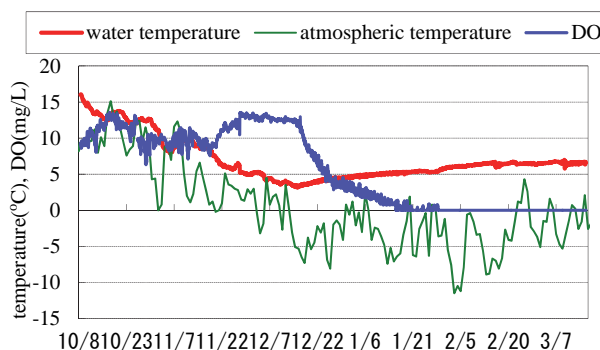


Fig.4 Result of self-recording instruments.

through December 1) and it was small and stable when the water temperature was lower than 5°C (after December 1). It was visually confirmed on December 9 that the river was not iced over, although ice sheets were floating in the river. On December 16, the river was mostly covered with ice, but a 50cm-wide stream of water was exposed on the both sides of the river. On December 24, the river froze over and the ice was thick enough for people to stand on. Thus, it is obvious that the variations in DO were significantly affected by river freezing.

b) Results of instrumental vertical observation

Figure 5 shows the results of vertical observation by means of immersion self-recording instruments. In the contour maps showing the observation results, dates are shown on the horizontal axis and water depths on the vertical axis. When the measurements were taken for the first time, on December 19, water

temperature(WT), DO, and turbidity(TB) were vertically uniform, suggesting that vertical circulation had taken place in the preceding autumn. It is likely that the freeze-over date was December 20, because the vertical distributions of the water temperature, the DO, and the turbidity began to vary on that day.

After the river froze over, the water temperature near the river surface decreased, and the water temperature near the bottom increased to gradually affect the water temperature upward. The water temperature varied within a range of 4°C vertically, and no distinct thermocline was observed. Downstream of the Kannon Bridge, municipal wastewater flows into the Barato River, increasing the bottom water temperature after the freeze-over of the river. The water temperature upstream of the bridge is also affected by the temperature of the wastewater, but the observation point of this study is 6km from the bridge. Thus, it is unlikely that heat is horizontally transported to raise the bottom water temperature near the observation point; the heat seems to be supplied by the riverbed. Geothermal heat and groundwater are the likely heat sources, but the details have not been determined.

The DO level decreased first in the bottom water layer, and the low-oxygen layer expanded upward. From February, DO was 3mg/L or lower at the depth of 3m or deeper. DO in the surface water layer decreased to 6mg/L, suggesting that ice was blocking the oxygen supply to the river water.

After the river froze over, the turbidity was greater in the bottom layer than in the surface layer. After the start of the observation, water in the surface layer became clearer, probably because suspended solids settled out. In contrast, the turbidity in the bottom layer increased after the start of the observation. Water samples collected from the bottom water layer were a clear yellowish-brown, which suggests the elution of iron. The color was not dark enough to indicate the presence of iron sulfide. It is presumed that the turbidity level in the bottom water layer increased because iron and settling particles were not fully deposited. This result regarding turbidity suggests that the disturbance of river water due to winds was prevented by the ice cover.

Water temperature and DO in and around the bottom water layer are different from the corresponding values shown in Fig.4. When the sensor was dropped into the river for instrument vertical observation, the air temperature was 15°C below zero and the water temperature was 4°C. Because of the temperature of the sensor, the temperature of the water mass around the sensor was not fully stabilized when measurements were taken. However, the measurements taken by the sensor show the overall variations in water temperature and DO.

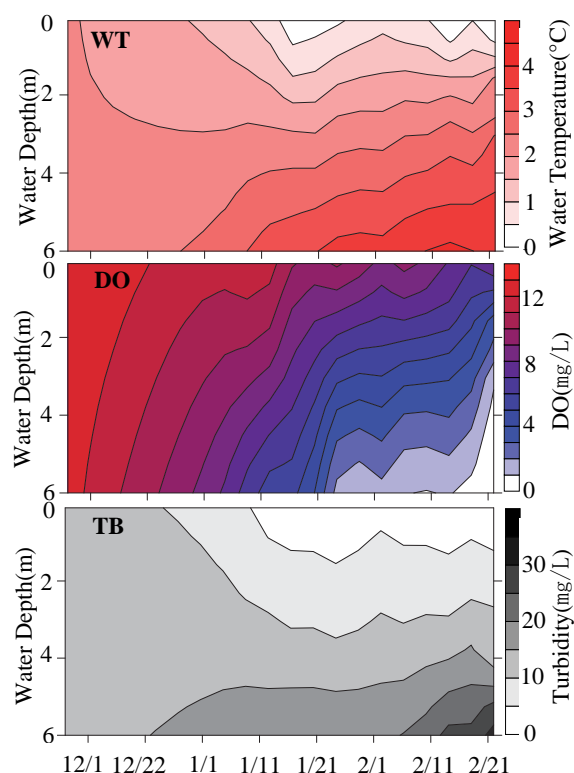


Fig.5 Results of vertical observation.

(3) Results of water sample analysis

The results of water quality analysis are shown in Fig.6 and Fig.7 in terms of time-series variations in the surface, middle and bottom water layers. When the observation started on December 9, no vertical variation was seen for any of the measurement items. The instrument observation results also show that the water quality is vertically uniform due to vertical circulation of water.

a) Organic matter indices

The analysis results concerning COD, BOD, and Chl-a, which are regarded as organic matter indices, are shown in Fig.6. COD was the highest in the bottom layer, though COD decreased in all three layers during the freeze-over period. Because COD in the bottom sediments was high (cf. Table 1) and the suspended solids settled out (cf. Fig.5), it is likely that persistent organic substances derived from suspended solids settled down.

BOD and Chl-a rapidly decreased after the freeze-over of the river and remained around the levels of the minimum determination limit during the freeze-over period. Due to the low water temperatures and decreased insolation, plankton productivity was reduced and easily decomposable organic substances did not increase.

b) Phosphorus

As shown in Fig.6, after the start of the observation, T-P decreased in the surface water layer and slightly increased in the bottom water layer. The

amount of decrease in the T-P level was larger in the surface layer than in the lower layers. $\text{PO}_4\text{-P}$ remarkably increased in the bottom layer.

On January 19, T-P and $\text{PO}_4\text{-P}$ in the bottom water layer spiked. In light of the COD levels, the sudden increase in T-P and $\text{PO}_4\text{-P}$ is presumed to have been caused by the settling of suspended solids.

Figure 6 also shows organic phosphorus (O-P) as calculated by subtracting the $\text{PO}_4\text{-P}$ level from the T-P level. Strictly speaking, the O-P level shown is the concentration of suspended solids and dissolved matter, rather than the concentration of organic matter alone. O-P was used for getting a rough idea of the variations in water quality. In the three layers, the rate of decrease in O-P was more or less the same. Because the rate of decrease in BOD was also similar in the three layers, it is presumed that the internal production of organic matter decreased.

Thus, it was confirmed that inorganic phosphorus increased first in the bottom water layer after the river froze over. The results of water sample analysis for phosphorus suggest that multiple phenomena were taking place, including the supply of phosphorus from settling solids, the elution of phosphorus from bottom sediment due to anoxic conditions in the bottom water layer, and the accumulation of $\text{PO}_4\text{-P}$ that was unused due to a decrease in the internal production of organic matter. Comparison of T-P and $\text{PO}_4\text{-P}$ among the three layers indicates that phosphorus was mainly supplied through elution from bottom sediment rather than through the decomposition and settling of suspended solids.

c) Nitrogen

As with T-P, T-N also decreased in the surface water layer and increased in the bottom water layer (**Fig.7**).

The $\text{NO}_3\text{-N}$ level in the three layers kept increasing until January 12, when it began to decrease. The increase in $\text{NO}_3\text{-N}$ from December 9 through January 12 is presumed to be from the supply of nitrogen by backflow. $\text{NH}_4\text{-N}$ increased due to the decomposition of organic matter. Because dissolved oxygen was abundant from December 9 through January 12, the nitrification of $\text{NH}_4\text{-N}$ by aerobic bacteria seems to be another reason for the increase in $\text{NO}_3\text{-N}$. After January 12, $\text{NO}_3\text{-N}$ decreased in the three layers with the decrease in DO. The decrease in $\text{NO}_3\text{-N}$ was the greatest in the bottom layer, and was greater in the middle layer than in the surface layer. $\text{NO}_2\text{-N}$ changed in conjunction with the change in $\text{NO}_3\text{-N}$, but $\text{NO}_2\text{-N}$ increased in the bottom layer in and after February. $\text{NH}_4\text{-N}$ increased in the three layers. The increase was the greatest in the bottom layer, and was greater in the middle layer than in the surface layer. Distinctive changes in $\text{NH}_4\text{-N}$ were observed in the bottom layer after January 12 (i.e., after the

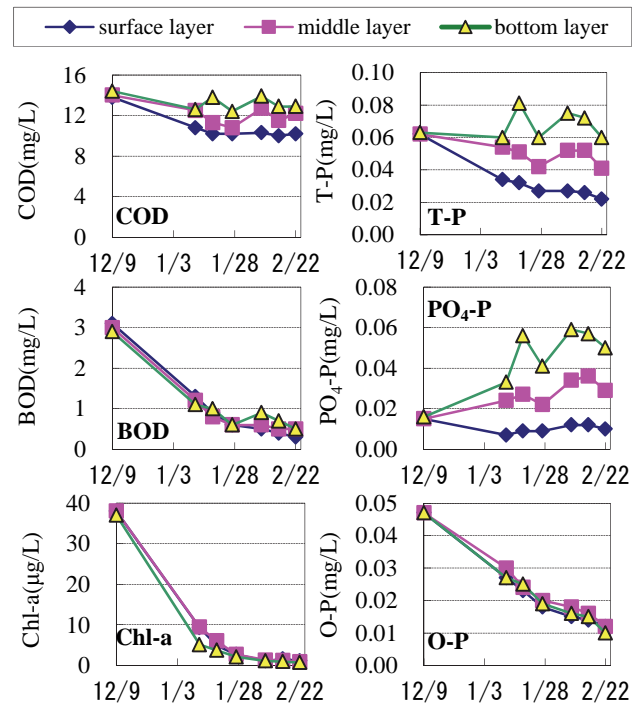


Fig.6 Results of COD, BOD, Chl-a, T-P, $\text{PO}_4\text{-P}$, O-P.

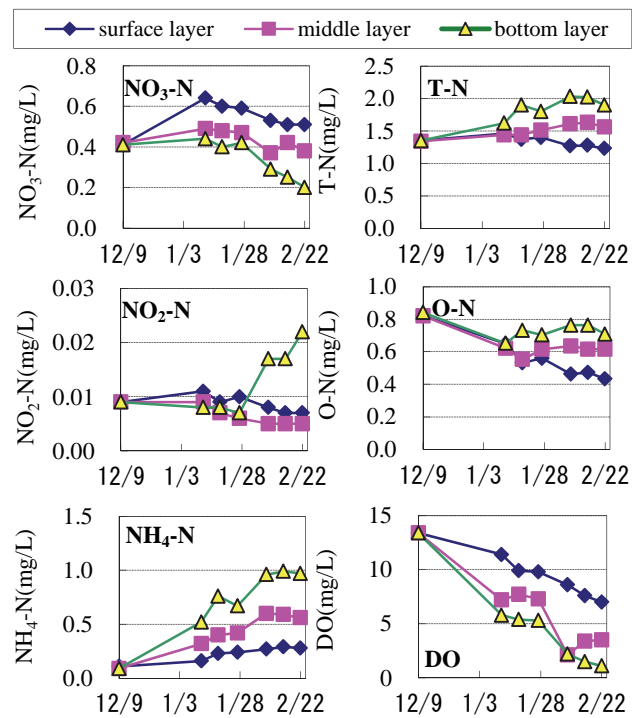


Fig.7 Results of $\text{NO}_3\text{-N}$, $\text{NO}_2\text{-N}$, $\text{NH}_4\text{-N}$, T-N, O-N, DO.

freeze-over of the river) and after February 8 (i.e., under anoxic conditions: cf. **Fig.4**). After the freeze-over of the river, $\text{NO}_3\text{-N}$ (i.e., an oxidizing substance) was transformed to $\text{NH}_4\text{-N}$ (i.e., a reducing substance). $\text{NO}_3\text{-N}$ was the lowest in the bottom water layer and was lower in the middle layer than in the surface layer. $\text{NH}_4\text{-N}$ was the greatest in the bottom layer and was greater in the middle layer than in the surface layer. This suggests that oxygen was first consumed in the bottom water layer. In the ob-

servation period, $\text{NO}_3\text{-N}$ and $\text{NH}_4\text{-N}$ decreased by 0.2mg/L and 0.9mg/L, respectively, in the bottom water layer. On the assumption that $\text{NO}_2\text{-N}$ can be ignored because it is lower than $\text{NO}_3\text{-N}$ and $\text{NH}_4\text{-N}$ by two orders of magnitude, it is presumed that nitrogen was supplied through elution rather than the transformation of $\text{NO}_3\text{-N}$ to $\text{NH}_4\text{-N}$.

Organic nitrogen (O-N) is calculated by subtracting the sum of $\text{NO}_3\text{-N}$, $\text{NO}_2\text{-N}$, and $\text{NH}_4\text{-N}$ from the T-N level. O-N markedly decreased in the surface layer in a way similar to the decrease in O-P, but O-N did not change significantly in other layers.

For reference, the results of water sample analysis for DO are also shown in Fig.7. Even though oxygen might have mixed into the water samples during collection, DO decreased. This result is consistent with the results shown in Fig.4 and Fig.5.

The data in Figures 4, 5, 6, and 7 show that the variations in water quality in the early part of the freezing period (i.e., December 20 through January 28) are different from those in the latter part (i.e., after January 28), which suggests that this difference in water quality variations is related to the development of an anoxic condition. It is necessary to reexamine the nutrient concentrations in water between the depth of water-sampling or of stationary instrument observation (i.e., 5m deep) and the bottom sediment (i.e., 6m deep). However, the variations in inorganic nutrient concentration indicate that nitrogen was mainly supplied through elution.

(4) Elution test results

In elution tests, the data obtained by analyzing water samples were put together as follows: $\text{PO}_4\text{-P}$ is referred to as I-P, and the combined $\text{NO}_3\text{-N}$, $\text{NO}_2\text{-N}$ and $\text{NH}_4\text{-N}$ is referred to as I-N below. The concentrations of I-P and I-N were calculated by subtracting the values of the samples used in a contrastive analysis from the values obtained by analyzing the samples in which water was exposed to bottom sediment. Variations in the quantity of organic matter due to increase or decrease of microorganisms and chemical decomposition of organic substances were negligible; thus, the concentrations shown in Fig.8 are the results of the matter exchange between water and bottom sediment.

These results indicate that I-P and I-N are eluted from the bottom sediments of St.A under anoxic conditions. The rate of change in I-P and I-N in the 30 day experiment period was $2.3 \times 10^{-3} \text{mg/L/day}$ and $6.3 \times 10^{-2} \text{mg/L/day}$, respectively. The experiment vessel was 18cm in diameter, and the volume of water used for the elution test was 22L; thus, the elution rate per unit area was $2.0 \text{mg/m}^2/\text{day}$ for I-P and $54.7 \text{mg/m}^2/\text{day}$ for I-N.

These elution test results were compared with the

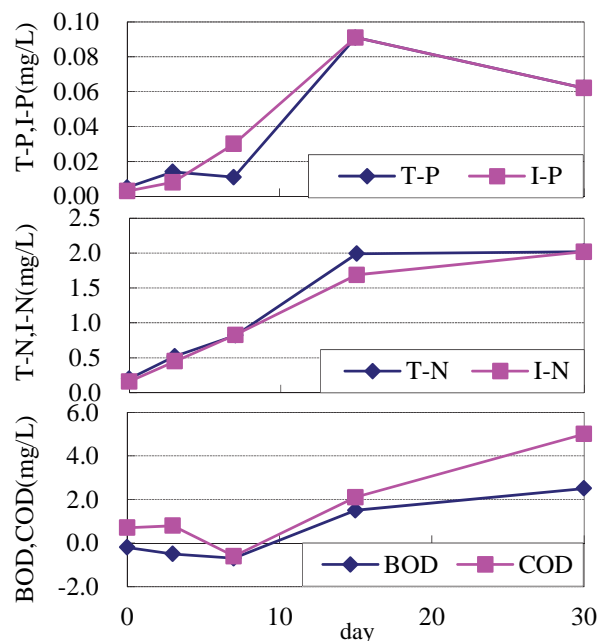


Fig.8 Results of elution test.

observation values for St.A shown in Fig.6 and Fig.7. The data used for comparison were the average concentrations of the three vertical water layers from January 12 through February 22, a period after the freeze-over of the river. The rates of change in the concentrations of I-P and I-N were $2.0 \times 10^{-4} \text{mg/L/day}$ and $6.4 \times 10^{-3} \text{mg/L/day}$, respectively. The reservoir capacity of the upper lake basin at the ordinary water level was 1.8 million m^3 , and at the bottom area was $3.0 \times 10^5 \text{m}^2$. Thus, the rates of change in the concentrations of I-P and of I-N were estimated at $1.2 \text{mg/m}^2/\text{day}$ and $38.4 \text{mg/m}^2/\text{day}$, respectively. In view of the fact that the temperature of the water used for the elution test was 15°C and the water of St.A was 4°C , the rate of elution estimated in the elution test is considered to be roughly in accordance with the field observation results. In other words, the laboratory elution test reproduced the actual phenomena in the upper lake basin. As the test was implemented under static, enclosed conditions, it is presumed that the surface water of the lake basin was not disturbed by winds or other causes for the duration of ice cover.

Additionally, the similarity in concentration between T-P and I-P and between T-N and I-N suggests that organic substances other than hydrocarbons were not eluted very much. Details are not known due to the lack of DOC observations. Because BOD and COD increased, it is necessary in the future to analyze the variations in DOC. The result of an elementary analysis of the samples on the 30th day of the experiment by Inductively Coupled Plasma Atomic Emission Spectroscopy (ICP-AES) showed that the concentration of iron had increased. It is

likely that the BOD and COD levels increased because bivalent iron promoted oxygen consumption. The concentration of phosphorus decreased from the 20th day through the 30th day of the experiment. It is possible that phosphorus became insoluble¹⁷⁾ under the influence of iron ions and pH change. The elution test results indicate that organic substances containing nitrogen and phosphorus were not eluted very much.

(5) Water quality for the duration of ice cover

When a river freezes over, the quality of river water begins to change because water is not exposed to air. After the Barato River froze, the water quality in the surface and bottom water layers obviously changed due to the sudden change in the way the river water was affected by heat, oxygen supply, and winds. Based on the observation and test results, the variations in the water quality of the Barato River are summarized as follows:

(a) When the river freezes over, the water temperature in the bottom water layer is stable and higher than the temperature of the surface water layer.

(b) DO decreases, causing an anoxic condition.

(c) The settling of suspended solids predominates; disturbance and resuspension of solids are suppressed.

(d) Internal production of organic matter is reduced, and easily decomposable organic matter decreases.

(e) The amount of inorganic nutrients (i.e., reducing substances) increases.

(f) A comparison between the field observation results and laboratory test results indicates that inorganic nutrients are supplied mainly through elution.

These findings suggest that variations in water quality during a freeze-over period in the water area where eutrophication has taken place are strongly influenced by the elution of nutrients and the development of anoxic conditions.

The nutrients accumulated under ice cover are vertically mixed after the breakup of ice, causing overgrowth of phytoplankton. However, when the increase in the annual mean air temperature in recent years is taken into account, it is presumed that shortening of the duration of ice cover leads to a reduction in accumulated nutrients. Consequently, plankton growth is inhibited. On the other hand, a rise in water temperature promotes plankton growth. It is necessary to understand how the inhibition and promotion of plankton growth affect water quality. In view of this, observation data on the water quality of public water bodies, which were provided to this study on a regular basis by the Sapporo Development and Construction Department, and data on air tem-

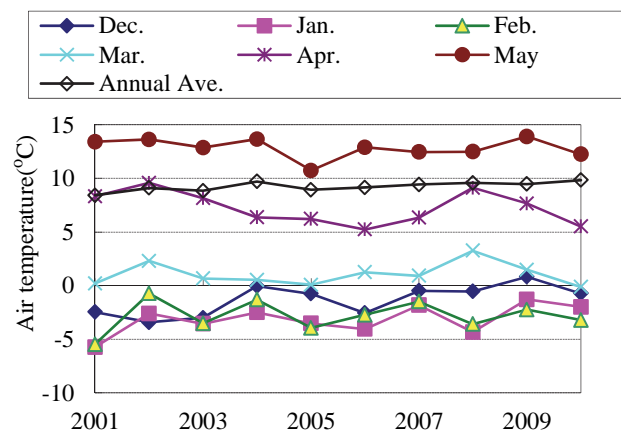


Fig.9 Change in air temperature at Ishikari.

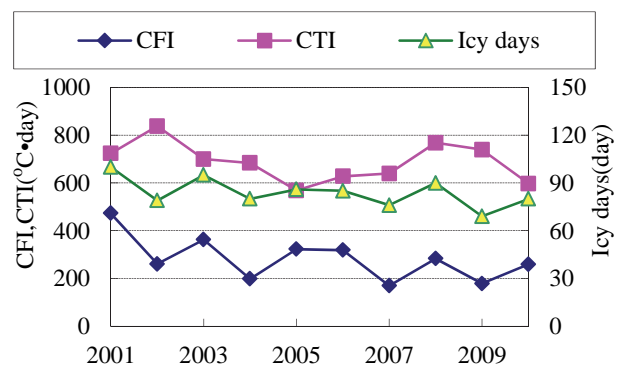


Fig.10 Changes in CFI, CTI, Icy days.

peratures collected from the Japan Meteorological Agency website were used for retrospectively analyzing the effects of climate change on water quality.

5. RELATIONSHIPS BETWEEN RIVER ICE COVER AND WATER QUALITY

(1) Variations in air temperature

Based on the air temperature data of Ishikari from 2001 through 2010, changes in the annual mean temperature, as well as in the monthly mean temperature from December through May, are shown in Fig.9. The annual mean temperature increased every year. According to the slope of a regression line, the rate of increase is $0.11^{\circ}\text{C}/\text{year}$. The monthly mean temperature in December and January increased noticeably, and the monthly mean temperature in April decreased. The monthly mean temperature in other months did not change in any specific way.

Figure 10 shows the changes in cumulative freezing index (CFI), cumulative thawing index (CTI), and the number of icy days. In calculating the CFI, absolute values of daily mean temperatures below zero were summed from November 1 through April 30. The CTI was calculated by summing absolute values of daily mean temperatures above the freezing point from January 1 through May 31.

Icy days per year have been decreasing year by year, indicating that the mean air temperature in winter has been increasing. Accordingly, the CFI value has been decreasing from year to year. The CTI value has been decreasing also, probably because of the decreasing monthly mean temperature in April. These results show that the monthly mean temperature has been increasing in December and January but has been decreasing in April, in contrast to the increase in annual mean temperature.

The rise in the winter air temperature is likely to affect the duration of ice cover, but freeze-over dates of the Barato River have not been recorded. Thus, freeze-over dates were retrospectively estimated based on an interview survey of public/industrial water consumers, photos taken during regular surveys, and the CFI value.

(2) Estimation of freeze-over and breakup dates

Figure 11 shows the changes in the number of freezing degree-days from 2001 through 2010. The dates of regular water quality surveys are shown by white circles. The photos taken every December at the time of a water quality survey show that the river was mostly ice-free. Even when the river was partly frozen, skim ice was floating as shown in **Photo 5**. In January every year, the river froze over and researchers were able to take measurements on the ice as shown in **Photo 6**. The freeze-over date is defined in this study as the date when the river freezes over and ice has become thick enough for people to stand on. In **Fig.11**, the greatest value of CFI in December is $28.6^{\circ}\text{C}\cdot\text{day}$, and that is defined as the maximum value of CFI during the time when the river is ice-free. The smallest value of CFI in January is $41.6^{\circ}\text{C}\cdot\text{day}$, and that is defined as the minimum value of CFI during the time when the river is covered with ice. The mean value of the maximum and the minimum values (i.e., $35.1^{\circ}\text{C}\cdot\text{day}$) is assumed to be the value of CFI on the day when the river freezes over. On a curve of the value of CFI each year, the date when $35.1^{\circ}\text{C}\cdot\text{day}$ is reached is assumed to be the freeze-over date.

Breakup dates are retrospectively estimated as follows: **Figure 12** shows the changes in the value of CTI from 2001 through 2010. The dates of regular water quality surveys are shown by white circles. In March every year, the river was frozen over as shown in **Photo 6**. At the time of a regular survey every April, ice in the river had broken up. It seemed possible to estimate a breakup date by using the value of CFI on April 30 in **Fig.11**, or by calculating the average value of the maximum value of CTI in March and the minimum value of CTI in April. However, the estimation results were not consistent with the observed situations and with the results of an inter-

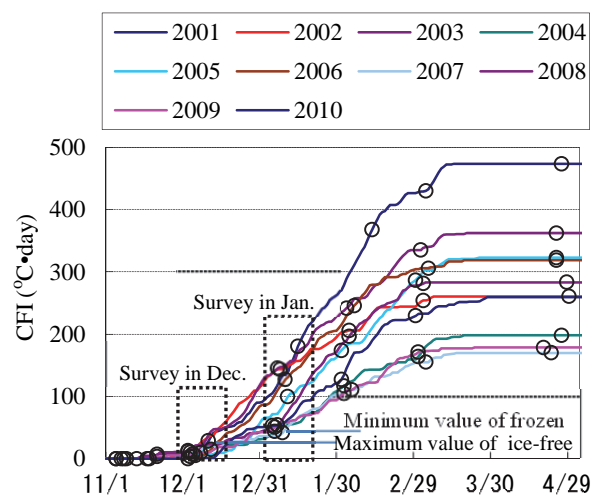


Fig.11 Changes in CFI and the survey date.



Photo 5 Survey in December (2007/12/3).

Photo 6 Survey in January (2009/1/6).

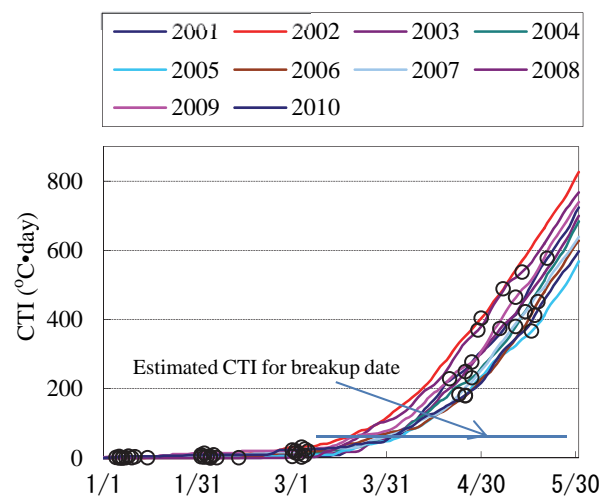


Fig.12 Changes in CTI and the survey date.

view survey of public/industrial water consumers. Thus, on the assumption that the value of CTI indicating breakup was equal to the value of CFI indicating freeze-up, namely, $35.1^{\circ}\text{C}\cdot\text{day}$, the breakup date in every year was retrospectively estimated as shown in **Fig.12**. The estimated breakup dates were consistent with the observations and with the interview survey results.

The estimated freeze-over/breakup dates and durations of ice cover are shown in **Table 2**. The freeze-over date estimated for 2010 was consistent

with the results of instrument observations. The duration of ice cover was the longest in 2003/04 winter and the shortest in 2009/10 winter. In 2009/10 winter, the freeze-up date was 16 days later than in 2003/04 winter; the breakup date was 11 days earlier than in 2003/04 winter and the duration of ice cover was 27 days shorter than in 2003/04 winter. In other words, the duration of ice cover has shortened by about one month in the last ten years.

(3) Relationships between the duration of ice cover and water quality

The trend in the variation in river water quality for the duration of ice cover was analyzed on the basis of the water quality data that had been regularly collected from 2001 through 2010. Water samples were collected at the depth of 1.2m (cf. Fig.2) on one day in the first, second, or third week of every month.

Based on the results of regular surveys during freeze-over periods, DO, $\text{NH}_4\text{-N}$, and $\text{PO}_4\text{-P}$ were chosen from the water quality data for examinations of the relationships between the duration of ice cover and the water quality. In the observation results, DO, $\text{NH}_4\text{-N}$, and $\text{PO}_4\text{-P}$ had vertical concentration gradients. In regular water quality surveys, data were collected only at the depth of 1.2m. Therefore, the results of the regular surveys are not sufficient for understanding the actual variations in water quality. Because the water quality in the frozen river was observed only in a single year, the relationships between the duration of ice cover and the water quality cannot be analyzed. However, long-term data from regular water quality surveys at a fixed water depth were accumulated, and these data indicated seasonal variations in the water quality. Thus, for the purpose of understanding the long-term trend in water quality, these data were used for analysis of the relationships between the duration of ice cover and the annual variations in water quality.

a) Variations in DO

Figure 13 shows the annual variations in DO. Initially, the annual variations in DO, $\text{NH}_4\text{-N}$, and $\text{PO}_4\text{-P}$ were compared between relatively warm years and cool years, but relationships between the variations in these levels and the duration of ice cover were not obvious because DO, $\text{NH}_4\text{-N}$, and $\text{PO}_4\text{-P}$ varied in different ways from year to year. The years 2005 and 2002 were used for identifying the characteristics of annual variation in DO, because the CFI value was the smallest in 2005 and the greatest in 2002 (Fig.10). Figure 13 shows that the concentration of DO decreased in the freeze-over period between December and March in these two years, although the DO level decreased differently in 2005 as compared with 2002. The DO concentration was the lowest in March. In the past ten years, DO in March

Table 2 The estimated freeze-over/breakup dates and durations of ice cover.

Year	Freeze-over date	Breakup date	Durations of ice cover (days)
2001	12/12	3/23	102
2002	12/11	3/9	89
2003	12/11	3/25	105
2004	1/3	3/23	81
2005	12/27	3/22	86
2006	12/16	3/17	92
2007	12/31	3/24	84
2008	12/25	3/16	83
2009	12/27	3/14	78
2010	12/21	3/19	89

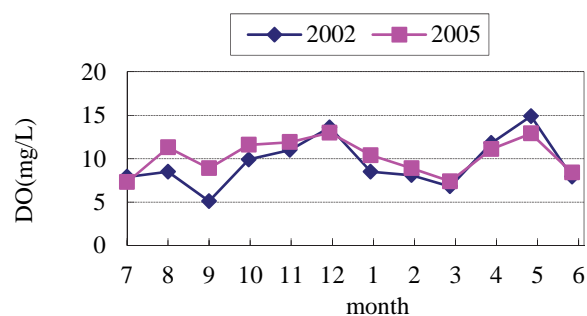


Fig.13 Annual variation in DO.

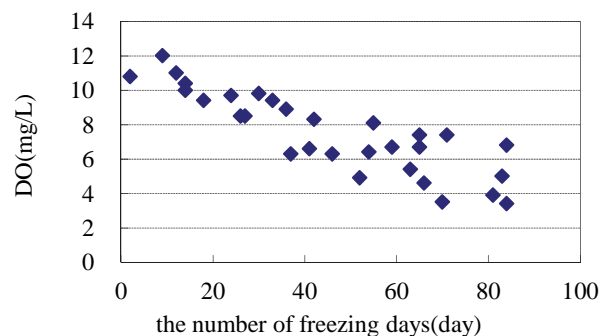


Fig.14 Relationship between DO and the number of ice cover days.

varied from year to year, and it had no clear relationship with the duration of ice cover (Table 2). Thus, the comparison of annual variation between the two years failed to clarify the changes in the water quality in relation to freeze-over dates, breakup dates, and dates of water quality surveys.

For the purpose of determining the relationship between the variations in DO and the duration of ice cover, a new variable was created on the basis of the estimated freeze-over/breakup dates shown in Table 2. Specifically, on the basis of Table 2, the number of days from an estimated freeze-up date to the date of a regular water quality survey was counted for January, February, and March. Figure 14 shows the relationships between DO as measured during regular water quality surveys and the number of days

counted (i.e., freezing days). In **Fig.14**, DO decreases with increase in the number of freezing days. This result suggests that the shortening of the duration of ice cover due to the recent rise in the mean air temperature mitigates the decline in DO.

b) Variations in $\text{PO}_4\text{-P}$

Figure 15 shows the annual variations in $\text{PO}_4\text{-P}$ in 2002 and 2005. The concentration of $\text{PO}_4\text{-P}$ began to increase in January, when the river froze over, and decreased sharply in April and May, after the breakup of ice. In the ten-year data, the peak concentration and the date when the peak concentration was reached varied from year to year, and no clear relationship was verified between $\text{PO}_4\text{-P}$ and the durations of ice cover shown in **Table 2**. This result is probably attributable to the fact that the week for the water quality survey was fixed for each of the 12 months; thus, the number of freezing days by the time of the water quality survey differed from year to year.

Figure 16 shows the relationships between $\text{PO}_4\text{-P}$ as measured during regular water quality surveys from January through March and the number of freezing days by the time of each survey. Data for April were not used because the data were collected after the breakup of ice and the water quality was likely to be affected by $\text{PO}_4\text{-P}$ supplied by snowmelt and disturbed bottom sediment. In **Fig.16**, $\text{PO}_4\text{-P}$ increases with increase in number of freezing days.

c) Variations in $\text{NH}_4\text{-N}$

Figure 17 shows the annual variations in $\text{NH}_4\text{-N}$ in 2002 and 2005. The concentration of $\text{NH}_4\text{-N}$ begins to increase in December and peaks in March. In the ten-year data, the peak concentration varies from year to year, and no clear relationship is confirmed between $\text{NH}_4\text{-N}$ and the durations of ice cover shown in **Table 2**.

Figure 18 shows the relationships between $\text{NH}_4\text{-N}$ as measured during regular water quality surveys from January through March and the number of freezing days by the time of each survey. In **Fig.18**, $\text{NH}_4\text{-N}$ increases with increase in the number of freezing days. This result and the variations in DO suggest that a longer duration of ice cover results in a longer duration of anoxic conditions in the bottom water layer as well as in an increased cumulative elution of $\text{NH}_4\text{-N}$. Thus, the shortening of the duration of ice cover is likely to cause a decline in the cumulative elution of $\text{NH}_4\text{-N}$.

These findings show that anoxic conditions develop and inorganic nutrients are eluted in the frozen river, and that the cumulative elution of $\text{NH}_4\text{-N}$ increases with increases in the number of freezing days. **Figure 14** suggests that the shortening of the duration of ice cover due to the recent rise in the mean air temperature inhibits the development of

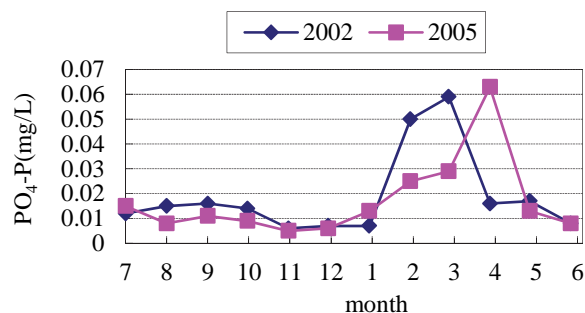


Fig.15 Annual variation in $\text{PO}_4\text{-P}$.

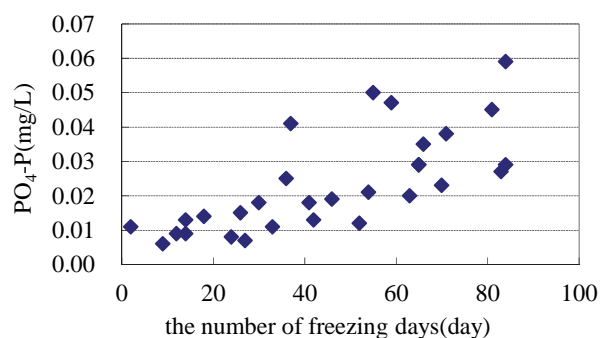


Fig.16 Relationship between $\text{PO}_4\text{-P}$ and the number of ice cover days.

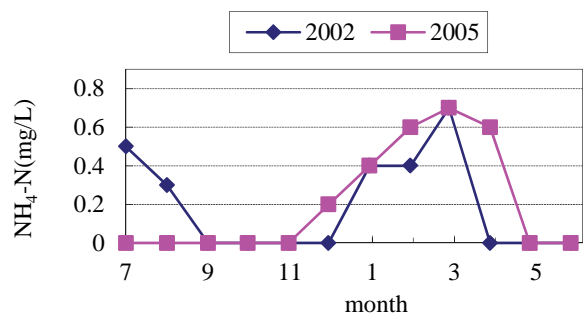


Fig.17 Annual variation in $\text{NH}_4\text{-N}$.

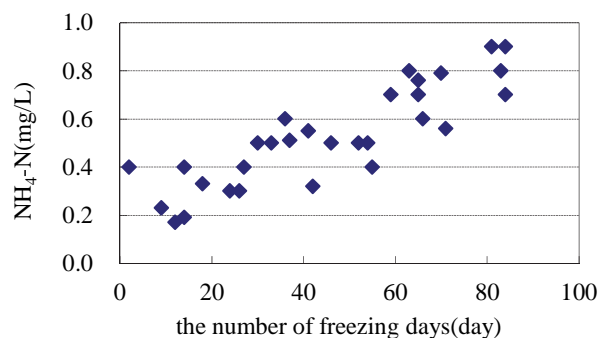


Fig.18 Relationship between $\text{NH}_4\text{-N}$ and the number of ice cover days.

anoxic conditions. Based on **Figures 16** and **18**, it is presumed that the cumulative elution of inorganic nutrients decreases even when nitrogen conversion is taken into account, because the cumulative elution of $\text{PO}_4\text{-P}$ and $\text{NH}_4\text{-N}$ decreases. Consequently, the quality of river water is improved for the duration of ice cover.

(4) Variations in water quality after the breakup of ice

a) Comparison of annual variations

Figures 19, 20, and 21 show the annual variations in water temperature, BOD and Chl-a. The annual variations in 2002 when the value of CTI is the greatest and the annual variations in 2005 when the value of CTI is the smallest are compared in these figures.

Water temperature, BOD, and Chl-a decreased for the duration of ice cover from January through March, and sharply increased after the breakup of ice in and after April. In April and May, the water temperature, BOD, and Chl-a were higher in 2002 than in 2005, except for Chl-a in May. Chl-a rose sharply in May 2005, to a level higher than in 2002. Because the relationships between the duration of ice cover and the water quality in April and May were not clearly understood, the variations in water quality after the breakup of ice were analyzed.

b) Relationships between the breakup dates and the water quality after the breakup of ice

Regular water quality surveys were conducted in the third week of April and the first week of May every year. In Fig.22, the number of days elapsed since each of the breakup dates shown in Table 2 until each date of the regular water quality surveys is related to the variations in water temperature, BOD, and Chl-a. The water temperature rose as the day went on after the breakup of ice. The BOD level continued to increase after the breakup of ice to reach its peak around the 60th day after the breakup, and then it decreased to 4-5mg/L and remained there, although it increased slightly around the 90th day. Although the pattern of variation in Chl-a is not very clear, Chl-a also peaked around the 60th day after the breakup, decreased afterward and then began to increase around the 90th day. Because regular water quality surveys are conducted on fixed dates every year, the number of days that elapse from the breakup of ice until a survey will increase if the duration of ice cover is reduced. A rise in the water temperature leads to an increase in the concentration of Chl-a and BOD in April and May, namely, during the 60 days after the breakup of ice. This seems to result in water quality deterioration.

The analysis results of water quality variations during the freeze-over period suggest that shortening of the duration of ice cover leads to a reduction in the volume of accumulated nutrient salts and thus to improvement of the river water quality. Observation results alone are not sufficient to determine whether a reduction in the duration of ice cover actually results in deterioration or improvement of water quality. The use of a simulation model seemed effective for examining the two opposite effects of the shortening of

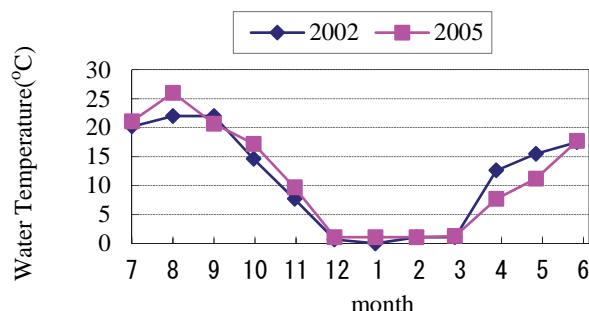


Fig.19 Annual variation in water temperature.

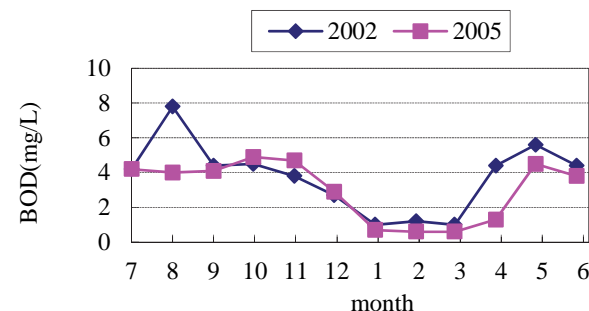


Fig.20 Annual variation in BOD.

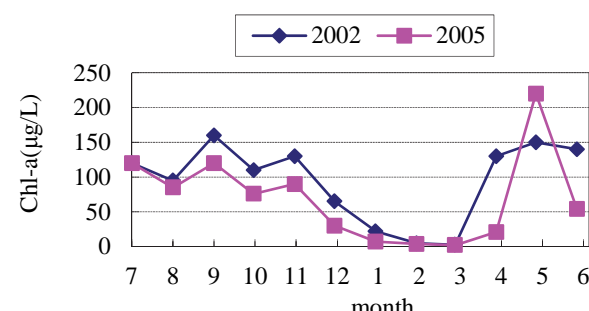


Fig.21 Annual variation in Chl-a.

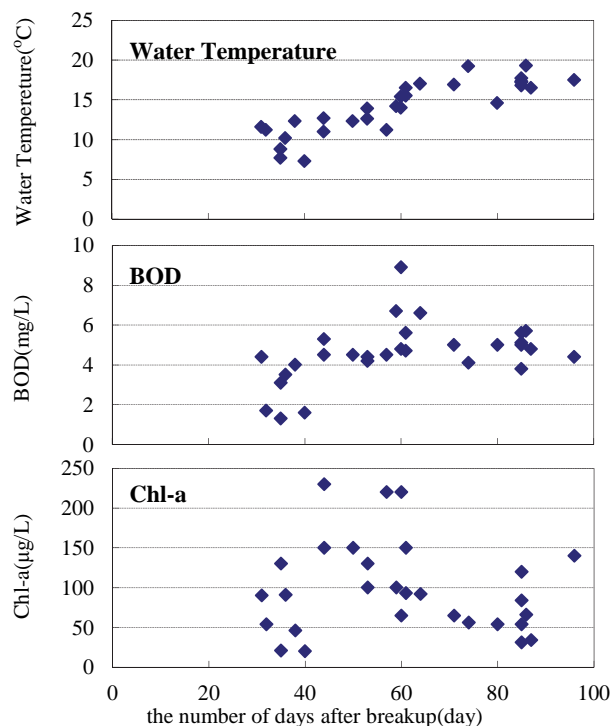


Fig.22 Relationship between the number of ice cover days and water temperature, BOD, Chl-a.

ice cover duration. Thus, a simulation model was developed for analyzing how freeze-over and ice breakup affected water quality.

6. WATER QUALITY SIMULATION MODEL

(1) Outline of the simulation model

For the purpose of predicting the water quality of the Barato River, the authors of this paper developed two-dimensional vertical ecosystem models that can simulate ice formation. Due to the lack of observation data on the water quality after the river froze over, vertical distribution profiles of nutrient salts and water temperatures were not known. Thus, the results of this study and of regular water quality surveys were used for developing an improved model.

Specifically, a two-dimensional simulation model¹⁸⁾ developed by Public Works Research Institute was improved to account for backflow in the flow calculation. In the simulated water area, meshes were generated by using vertical rectangular coordinates. In the two-dimensional vertical meshes, the material cycle, particularly the cycle of phytoplankton, was simulated as shown in **Fig.23**. Each mesh is 0.5m wide in the direction of the z-axis and 500m wide in the direction of the x-axis. To reproduce the state of ice cover, the heat balance shown in **Fig.24** was simulated in the meshes of the surface water layer. For simplicity, it was assumed that the ice cover was 0m or 0.5m thick, and that a 0.5m layer of surface water became ice cover at water temperatures of 0°C

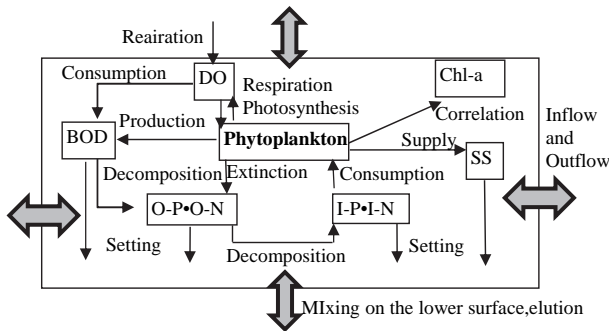


Fig.23 Conceptual scheme of eco-system model.

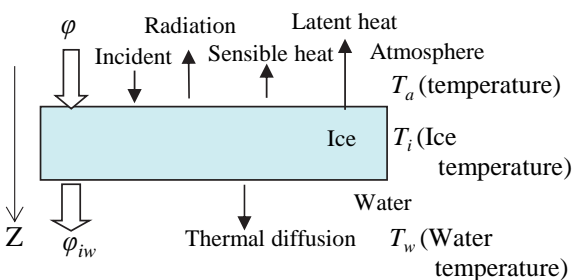


Fig.24 Heat balance scheme at surface.

or lower and became water mass when the temperature of ice in the surface layer rose to 0°C or higher. Temperature variations within ice layers were not taken into account. The basic equations are shown below:

a) Equation of continuity

$$\frac{\partial u}{\partial x} + \frac{\partial v}{\partial z} = 0 \quad (1)$$

In the equation above:

x, z : the coordinates in the flow direction and the vertical direction (m);

u, v : the flow velocities in the flow direction and the vertical direction (m/s);

b) Equations of motion

In the flow direction:

$$\begin{aligned} \frac{\partial u}{\partial t} + u \frac{\partial u}{\partial x} + v \frac{\partial u}{\partial z} = \\ - \frac{1}{\rho_0} \frac{\partial P}{\partial x} + \frac{\partial}{\partial x} \left(D_{mx} \frac{\partial u}{\partial x} \right) + \frac{\partial}{\partial z} \left(D_{mz} \frac{\partial u}{\partial z} \right) \end{aligned} \quad (2)$$

In the vertical direction:

$$\frac{\partial P}{\partial z} = -\rho g \quad (3)$$

In these equations:

ρ_0 : standard density (1,000kg/m³);

ρ : density of flowing water (kg/m³), which is a function of SS and water temperature;

P : water pressure (kg/m²);

D_{mx} : coefficient of momentum diffusion in the flow direction (m²/s), defined by using Richardson's 4/3 law¹⁹⁾;

D_{mz} : coefficient of momentum diffusion in the vertical direction (m²/s), which is a function of the Richardson number²⁰⁾;

g : gravitational acceleration (9.8m/s²);

c) Heat balance equation

$$\begin{aligned} \frac{\partial T}{\partial t} + u \frac{\partial T}{\partial x} + v \frac{\partial T}{\partial z} = \\ \frac{\partial}{\partial x} \left(D_{Tx} \frac{\partial T}{\partial x} \right) + \frac{\partial}{\partial z} \left(D_{Tz} \frac{\partial T}{\partial z} \right) + \phi \end{aligned} \quad (4)$$

In the equation above:

T : water temperature (K);

D_{Tx} : coefficient of temperature diffusion in the flow direction (1.4×10⁻⁷ m²/s);

D_{Tz} : coefficient of temperature diffusion in the vertical direction (1.4×10⁻⁷ m²/s);

C_w : specific heat of water (4,218 J/K/kg);

ϕ : heat flux (K/s);

Calculation of the heat flux is shown by Equation (9) below.

d) Equation of water quality component balance

Basic Equation (5) below is used for calculations regarding water quality components.

$$\begin{aligned} \frac{\partial X}{\partial t} + u \frac{\partial X}{\partial x} + (v + v_x) \frac{\partial X}{\partial z} \\ = \frac{\partial}{\partial x} \left(A_x \frac{\partial X}{\partial x} \right) + \frac{\partial}{\partial z} \left(A_z \frac{\partial X}{\partial z} \right) + \frac{\partial S(X)}{\partial t} \end{aligned} \quad (5)$$

In the equation above:

X : density of each water quality component (g/m^3);
 A_x, A_z : diffusion coefficients in the horizontal and vertical directions²¹⁾ (m^2/s);

v_x : settling velocity of each water quality component;

$S(X)$: the amount of biochemical change in matter X (g/m^3);

e) Basic equations for the amount of biochemical change in plankton

Taking plankton as an example of matter, basic equations for the amount of biochemical change are shown in (6) to (8) below:

$$\frac{\partial S(P_{all})}{\partial t} = \sum_{i=1,3} \{ (G_{Pi} - D_{Pi}) P_i \} \quad (6)$$

$$G_{Pi} = \beta_s \cdot \mu_{\max_i} \left\{ \frac{T}{T_{Si}} \exp \left(1 - \frac{T}{T_{Si}} \right) \right\}^3 \quad (7)$$

$$\frac{I_Y}{I_{Si}} \exp \left(1 - \frac{I_Y}{I_{Si}} \right) \cdot \frac{C_{IN}}{K_{INi} + C_{IN}} \cdot \frac{C_{IP}}{K_{IPi} + C_{IP}}$$

$$D_{Pi} = R_{ppi} \theta^{(T-20)} \quad (8)$$

In these equations:

$S(P_{all})$: variation in density of total plankton (cell/m^3);

P_i : plankton density by species (cell/m^3);

i : phytoplankton species (1: diatom; 2: green algae; 3: blue-green algae);

G_P : reproduction rate of phytoplankton (1/s);

β_s : space limitation factor (1.0);

μ_{\max} : maximum reproduction rate of plankton by species (diatom: 0.85 1/s; green algae: 0.64 1/s; blue-green algae: 0.70 1/s);

C_{IN} : I-N density (g/m^3);

C_{IP} : I-P density (g/m^3);

K_{IN} : Michaelis constant of nitrogen uptake (diatom: 0.25 g/m^3 ; green algae: 0.25 g/m^3 ; blue-green algae: 0.25 g/m^3);

K_{IP} : Michaelis constant of phosphorus uptake (dia-

tom: 0.002 g/m^3 ; green algae: 0.004 g/m^3 ; blue-green algae: 0.006 g/m^3);

D_P : phytoplankton mortality rate (1/s);

R_{pp} : phytoplankton mortality coefficient (0.13 1/s for the three algal species);

θ : temperature coefficient for phytoplankton mortality rate (1.04);

T : water temperature ($^{\circ}\text{C}$);

T_s : optimum water temperature (Diatom: 15 $^{\circ}\text{C}$; green algae: 20 $^{\circ}\text{C}$; blue-green algae: 25 $^{\circ}\text{C}$);

I_Y : solar radiation ($\text{cal/cm}^2/\text{day}$);

I_s : optimum solar radiation (300 $\text{cal/cm}^2/\text{day}$ for the three algal species);

The methods for determining the above-mentioned parameters, as well as for calculating the amount of biochemical change of other matter, are explained in a separate paper¹⁵⁾.

(2) Simulation of freeze-over conditions

a) Balance of heat transferred between air and ice cover

On the basis of the techniques developed by Kondo,²²⁾ the heat balance in the surface water layer was simulated as shown in **Fig.24**. The heat flux, or the heat transfer rate per unit area of the interface between atmosphere and ice cover, was calculated by the following Equations (9)-(20):

$$\phi = \frac{A}{\rho_i C_i} \{ (1-\alpha) S \downarrow + L \downarrow - \varepsilon \sigma T_i^4 - H - lE \} \quad (9)$$

$$L \downarrow = \varepsilon \sigma T_i^4 \left\{ 1 - \left(1 - \frac{L_d \downarrow}{\sigma T_i^4} \right) C \right\} \quad (10)$$

$$L_d \downarrow = (0.74 + 0.19x + 0.07x^2) \sigma T_i^4 \quad (11)$$

$$x = \log_{10}(0.14e_a) \quad (12)$$

$$e_a = e_{sat} \times RH / 100 \quad (13)$$

$$e_{sat} = 6.107 \times 10^{9.5T_i / (265.3 + T_i)} \quad (14)$$

$$C = 0.826D^3 - 1.234D^2 + 1.135D + 0.298 \quad (15)$$

$$C = 0.2235 \quad (D = 0) \quad (16)$$

$$D = N / N_0 \quad (17)$$

$$H = C_p \rho_a C_H u_a (T_i - T_a) \quad (18)$$

$$lE = l \rho_a \beta C_H u_a \{ e_{sat} - e_a \} \frac{0.622}{P} \quad (19)$$

$$\rho_a = 1.293 \cdot \frac{273.15}{273.15 + T_a} \left(\frac{P}{101325} \right) \left(1 - 0.378 \frac{e_a}{P} \right) \quad (20)$$

In these equations;

ϕ : the heat flux between atmosphere and ice cover (K/s);

S_{\downarrow} : the amount of global solar radiation (W/m²);

L_{\downarrow} : the amount of downward long-wave radiation (W/m²);

A : surface area (m²);

ρ_i : density of ice (914kg/m³);

C_i : specific heat of ice (2,100J/K/kg);

T_i : ice temperature (K);

T_a : air temperature (K);

α : albedo of ice surface (0.90);

ε : emission rate (1.00);

σ : Stefan-Boltzmann constant (5.67×10⁻⁸W/m²/K⁴);

H : sensible heat (W/m²);

LE : latent heat (W/m²);

$L_{d\downarrow}$: the amount of clear-sky downward long-wave radiation (W/m²);

e_a : water vapor pressure (hPa);

e_{sat} : saturated water vapor pressure on the ice surface (hPa);

RH : relative humidity (%);

C : function of cloud cover;

N : duration of sunshine (h);

N_0 : hours of daylight (h);

D : sunshine rate;

l : latent heat of sublimation of ice (2.83×10⁶ J/kg);

β : vaporization efficiency (1.0 according to condensation conditions);

C_p : specific heat of air at constant pressure (1,004J/kg/K);

ρ_a : air density (kg/m³);

C_H : bulk coefficient (1.2×10³);

u_a : wind velocity (m/s);

P : atmospheric pressure (hPa);

b) Balance of heat transferred between water and ice cover

Ice layer bottom flow is used for estimating the heat transfer coefficients of ice and water²³⁾. However, static water was assumed for the Barato River because the flow velocity in summer was around 0.03m/s, water flowed downstream or upstream alternately, and no observation data were available regarding freeze-over periods. Thus, the heat flux between ice cover and water was calculated by the heat transfer Equation (21), and the thermal diffusion coefficient was calculated by using physical properties and Equation (22). A heat conduction equation uses the quantity of heat supplied to a given space. In this paper, a one-dimensional heat conduction equation was applied to the vertical direction expressed in Equation (21).

$$\phi_{iw} = \frac{\partial}{\partial Z} \left(K_{iz} \frac{\partial T}{\partial Z} \right) \cong \frac{1}{\Delta Z} \left(K_{iz} \frac{T_i - T_w}{\Delta Z} \right) \quad (21)$$

$$K_{iz} = \frac{\lambda}{\rho_w C_w} \quad (22)$$

In these equations;

T_i : ice temperature (K);

T_w : water temperature (K);

ΔZ : layer thickness (0.5m);

ρ_w : water density (1,000kg/m³);

C_w : specific heat of water (4,180J/K/kg);

λ : heat conductivity at 0°C (0.561W/m/K);

K_{iz} : coefficient of thermal diffusion from ice to water (1.34×10⁻⁷ m²/s);

(3) Effects of ice cover on water quality components

To simulate ice cover conditions for estimating how ice cover affects the water quality components, the following conditions were assumed: load of bottom sediment disturbance = 0g/s; reaeration to increase the DO level = 0g; and heat supply to the bottom surface per unit area = 6.7×10⁻⁸ K/m²/day (according to the rate of increase in water temperature for the bottom water layer in St.A, 0.02K/day (Fig.5)). Additionally, the elution rates of inorganic nutrients that suggested freeze-over of the Barato River were assumed to be 1.2mg/m²/day for I-P and 38.4mg/m²/day for I-N (cf. Figures 6, 7, and 8). These elution rates are different from those previously estimated¹⁵⁾, because the water temperature is low and varies only slightly for the duration of ice cover in the Barato River. The elution rates for the duration of ice cover were assumed to be constant. Under ice-free conditions in summer, the elution rate is a function of water temperature and DO level¹⁵⁾.

Ice cover and snow accumulated on river ice are likely to reduce the impact of winds on water, as well as the penetration of light deep into water, although no observation results have verified this. Therefore, it was assumed that the impact of wind velocity was negligible for the interface between ice and water mass but was taken into account for the interface between air and ice. It was also assumed that no light penetrated into water beneath ice for the duration of ice cover, and that the intensity of solar radiation entering the water was 0 J/m²/day.

(4) Reproduction calculations

The simulation model developed in this study was used for reproducing the variations in water quality for the duration of ice cover, which were understood based on the survey results. Reproduction calculations were conducted from July 1, 2000 through December 31, 2010. Input data on weather conditions, interface levels, inflow, etc. were based on observation values reported in the past^{14), 15), 24), 25)}.

The initial conditions of calculations were determined on the basis of the regular water quality survey conducted in June 2000. There is one fixed point for water quality measurement in each of the three sections of the Barato River, namely, the section from the Shibi Canal to Kannon Bridge, the section from Kannon Bridge to Yamaguchi Bridge, and the upper lake basin (cf. **Fig.1**). Observation values in these sections were used as input values of water in both horizontal and vertical directions in calculations.

Regarding the interface between water and sediment, variations in sediment were ignored, and it was assumed that disturbed sediment and eluted nutrient salts were supplied to the meshes corresponding to the bottom water layer and that sediment was not contained in other meshes. As for the interface between ice and water mass, it was assumed that friction was negligible in determining whether the river was frozen over on the basis of calculations, and that the meshes corresponding to the surface water layer, after becoming solid, had no interactions with the underlying water layer in terms of mass transfer or transport. The surface water layer, after becoming liquid in a thawing period, was assumed to have the same water quality as the underlying water layer.

a) Time-series reproduction of water quality in the bottom layer

Regarding the water quality of the bottom layer at the depth of 5m in the winter of 2010, survey results and calculation results are compared as described below. In **Fig.25**, the calculation results concerning the water temperature and the DO level are compared with the measurements taken by the continuous self-recording instruments. The calculation results and water quality analysis results are compared for I-P and IN in **Fig.26**. In **Fig.25**, the water temperature and the DO level are approximately simulated. On and after December 16, the simulated water temperatures are about 2°C lower than the measured water temperatures. In the simulation, computational meshes at the depth of 6m were given heat, but the rise in the water temperature shown in the observation results after the breakup of ice was not reproduced. The reason that the rise in water temperature was not reproduced is probably because the vertical flow velocity was not high enough and the thermal diffusion coefficient was too small in the simulation. This result suggests the existence of vertical flow in the bottom water layer of the ice-covered river. The measurement results (cf. **Fig.5**) indicate the possibility of groundwater discharge from the riverbed, although the details are not known.

The DO level was approximately simulated, although the date when an anoxic condition was reached at the depth of 5m in the survey was January 30, while the corresponding date in the simulation

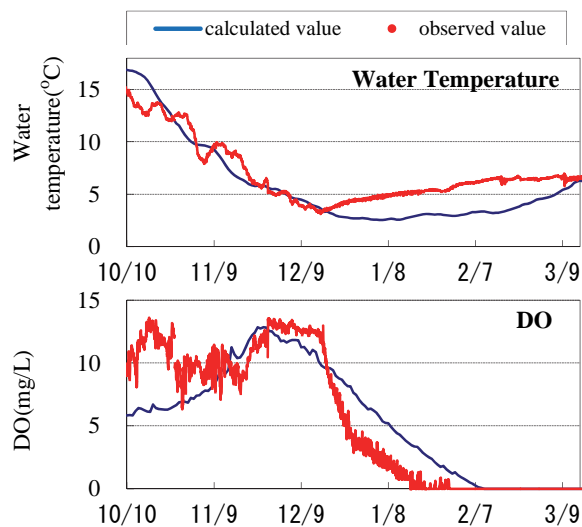


Fig.25 Reproduction of water temperature and DO in the bottom layer.

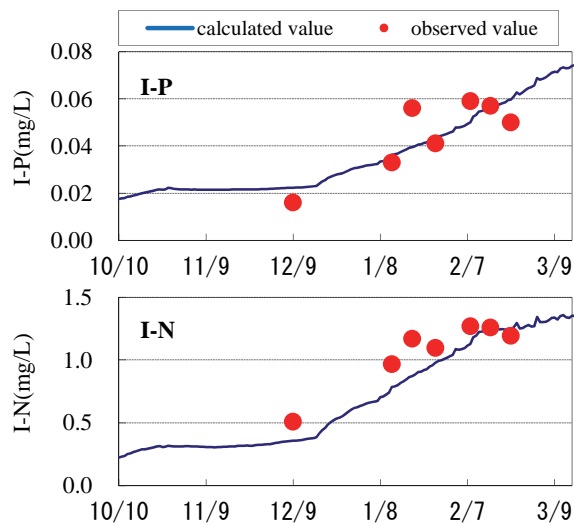


Fig.26 Reproduction of I-P and I-N in the bottom layer.

was a week later, February 7. In general, the overall trend, the water temperature, and the DO level were simulated with satisfactory accuracy.

In **Fig.26**, I-P and I-N at the depth of 5m are approximately simulated. According to the simulation result, I-P and I-N began to increase on December 16 when an anoxic condition developed in the meshes in the bottom layer at the depth of 6m where I-P and I-N were eluted.

Thus, the simulation model successfully reproduced the conditions in the frozen river where an oxygen-free condition develops in the bottom water layer and the concentrations of I-P and I-N increase due to elution. The water quality of the Barato River after it froze over was simulated fairly well. The simulation process suggests that an anoxic condition begins to develop in the bottom water layer when the Barato River freezes over.

b) Reproduction of the vertical profile of water quality components

Survey results and calculation results were also compared to determine how well the simulation model could reproduce the vertical profile of the water temperature and the levels of DO, I-P, and I-N. In **Fig.27**, calculation results are compared with the measurements taken by immersion-type self-recording instruments on February 15, 2010.

In **Fig.28**, calculation results are compared with the analysis results of water sampled on February 15, 2010. Because water at the depth of 0m-0.5m from the river surface is assumed to be frozen in the simulation, the values of water temperature and the levels of DO, I-P, and I-N are 0. Although a concentration gradient appears to be generated in the surface layer, calculations are based on the assumption that mass transfer does not take place between water and ice. **Figures 27** and **28** show that the simulation model successfully simulates a vertical profile of the water temperature, as well as of the levels of DO, I-P, and I-N.

c) Time-series reproduction of water quality in the surface layer

Calculation results and observation data on the water quality in public water bodies were compared to determine how well the simulation model reproduces the water quality in the surface water layer. Because the data on the water quality in public water bodies were collected on a monthly basis at the water depth of 1.2m, the data were compared with the calculated values for a water layer at the depths of 1.0-1.5m. The items for comparison were the water temperature, and the levels of BOD, Chl-a, I-P, and I-N. The simulation results are shown in **Fig.29**. As shown in **Fig.29**, the observation results of all items were approximately simulated, and the time-series variations from summer to the freezing season and then to the thawing season are reproduced well. Since 2007, water has been channeled from other rivers to increase the clarity of the water in the Barato River, and the simulation model took into account the effects of water from other rivers.

The freeze-over dates and breakup dates that were estimated on the basis of the calculated surface water temperatures agreed with the estimated dates of freeze-over and breakup shown in **Table 2** within a margin of error ± 5 days.

The water temperature of 15°C is significant in understanding the variations in BOD, Chl-a, I-P, and I-N in the simulation. In the simulation model, the optimum temperature for diatom growth was set at 15°C; thus, the plankton growth rate (cf. Equation (7)) was assumed to change when the water temperature decreased or increased to 15°C. The material cycle simulated in the model is as follows: When the

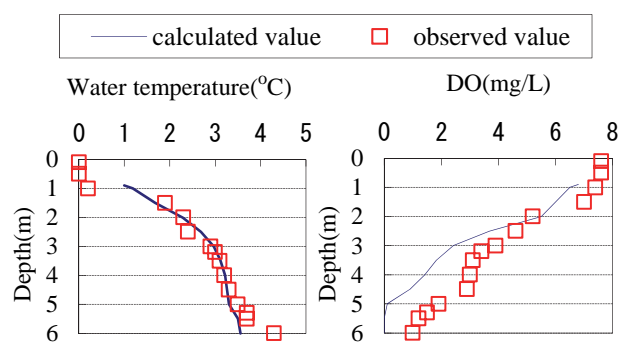


Fig.27 Reproduction of the vertical profile of water temperature and DO on February 15.

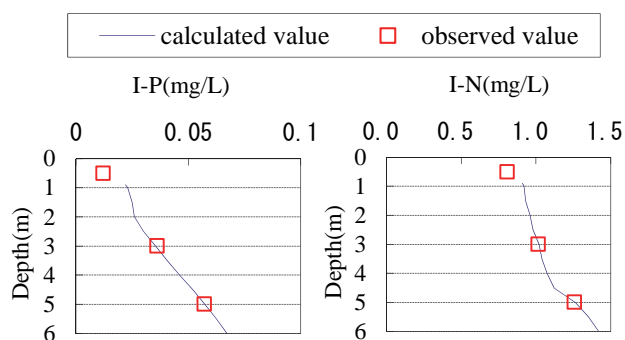


Fig.28 Reproduction of the vertical profile of I-P and I-N on February 15.

water temperature drops below 15°C in November, Chl-a decreases due to the death of plankton. Consequently, consumption of inorganic nutrients decreases, and I-N and I-P increase. Because of the reduction in the plankton population, as well as in the amount of photosynthesis, the BOD level also decreases. When the river freezes over in December, elution of inorganic nutrients significantly increases, thereby increasing I-N and I-P. In March when river ice breaks up, the water temperature and the plankton population increase, which result in increases in Chl-a and BOD and in decreases in I-N and I-P. Because plankton growth is promoted in May, when the water temperature rises to 15°C or higher, Chl-a and BOD increase sharply, and I-N and the I-P decrease rapidly. When I-N is exhausted afterward, the plankton population stops growing and begins to die, and BOD decreases. The material cycle simulated by the model is consistent with the observation data; thus, the simulation model seems to have successfully reproduced the water quality in the surface layer of the Barato River.

The comparison between the observation results and the simulated results verified that the simulation model was capable of reproducing spatiotemporal phenomena. Time-series predictions of the freeze-over, the breakup, and the water quality of the Barato River are now possible by using the simulation model.

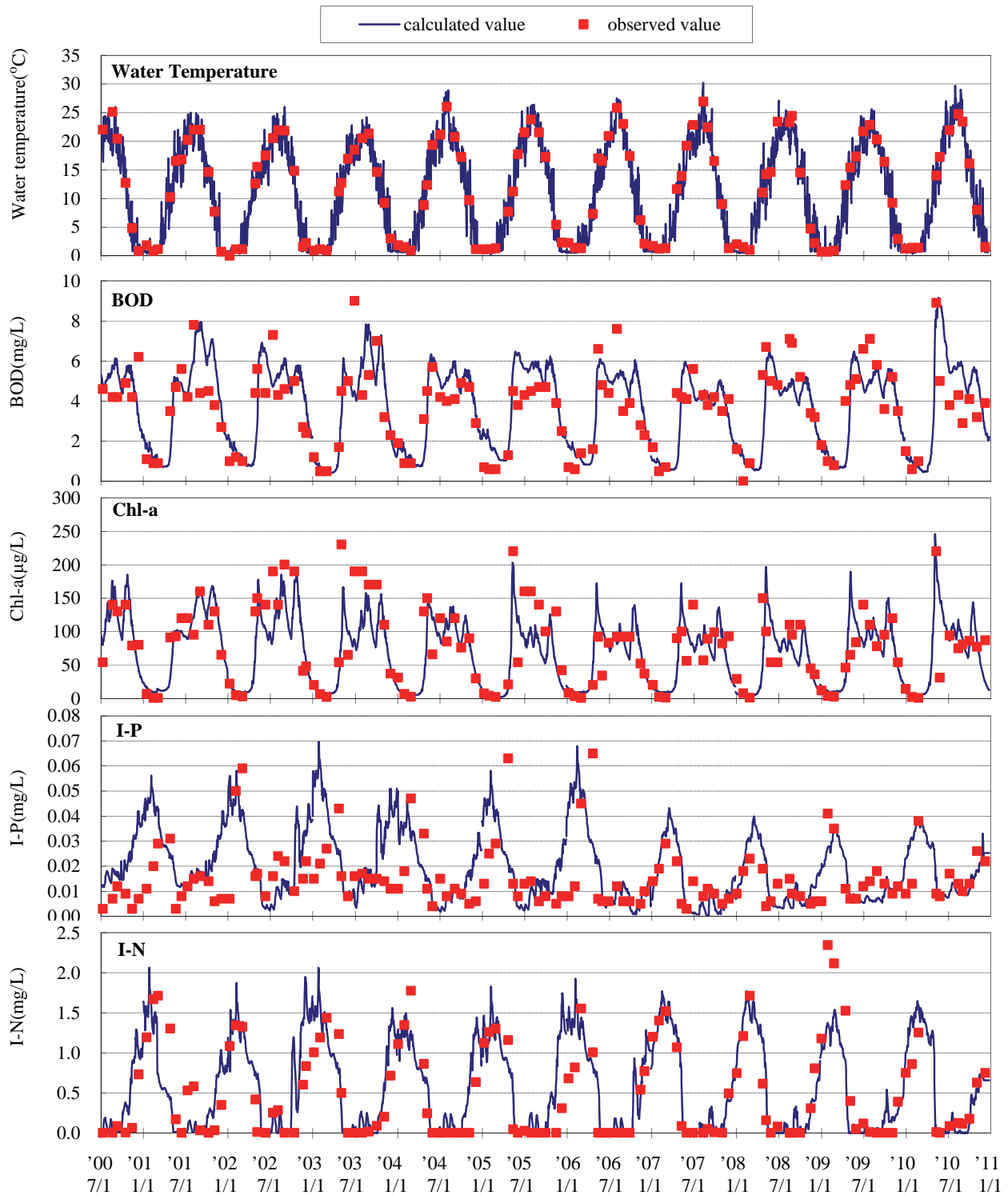


Fig.29 Reproduction of water quality in the surface layer.

7. EFFECTS OF CLIMATE CHANGE ON WATER QUALITY

To understand the effects of climate change on the water quality of the Barato River, the simulation results shown in Fig.29 were compared with each other. Particular focus was put on analyzing responses to climate change in terms of the timing of freeze-up dates and breakup dates. For 2002, the year

when the value of CTI was the greatest, and 2005, the year when the value of CTI was the smallest, the calculated values of BOD, Chl-a, I-P, and I-N are shown in Fig.30. Because the meteorological data and the inflow load data used for calculations were measured values, the load balance and the rainfall vary according to the year. Consequently, quantitative evaluation has not been conducted.

It should be noted that there is a difference of

about 12 days between 2002 and 2005 in terms of the date when the sharp decrease in inorganic nutrients and the sharp increase in BOD and Chl-a took place, around the beginning of May. In **Table 2**, the breakup date in 2002 differs from the breakup date in 2005 by 13 days, which suggests that the relationships between the duration of ice cover and the concentrations of water quality components were adequately simulated by the model. Chl-a peaked earlier in 2002 (May 1) than in 2005,

but the peak was higher in 2005 than in 2002. It is likely that the simulated Chl-a level was affected strongly by the water temperature, because the concentrations of inorganic nutrients were similar in 2002 and 2005 during the thawing period. On the other hand, the BOD peak in May is slightly higher in 2002 than in 2005. This suggests that the effects of climate change on water quality vary depending on the water temperature during and after the thawing period. Regarding the Barato River, however, water quality data during thawing periods have not been collected, snowmelt load has not been estimated and the effects of disturbed bottom sediment on water quality during thawing periods have not been observed. Additionally, as shown in **Fig.29**, the simulation model is not capable of accurately reproducing observation data; thus, accuracy of the model needs improvement. Because the simulation model approximately reproduces the observation results, it will be possible to use it for quantitative evaluation by taking sensitivity analysis and more diverse conditions into account.

8. CONCLUSION

The findings from this paper are summarized below:

(1) The results of laboratory experiments and water quality observations for a frozen river show that inhibition of reaeration under the ice-cover condition is followed by the development of an anoxic condition and the elution of inorganic nutrients. The amount of organic matter does not increase, and suspended solids are not supplied by disturbance of the bottom sediment in the frozen river.

(2) The durations of ice cover were estimated on the basis of the number of freezing degree-days and the number of thawing degree-days. The estimation results indicate that the rise in the annual mean air temperature has caused a reduction in the duration of ice cover.

(3) It is also suggested that the shortening of the duration of ice cover leads to a reduction in the amount of inorganic nutrient elution.

(4) Because the ice breaks up earlier than before, the water temperature and BOD in May have been

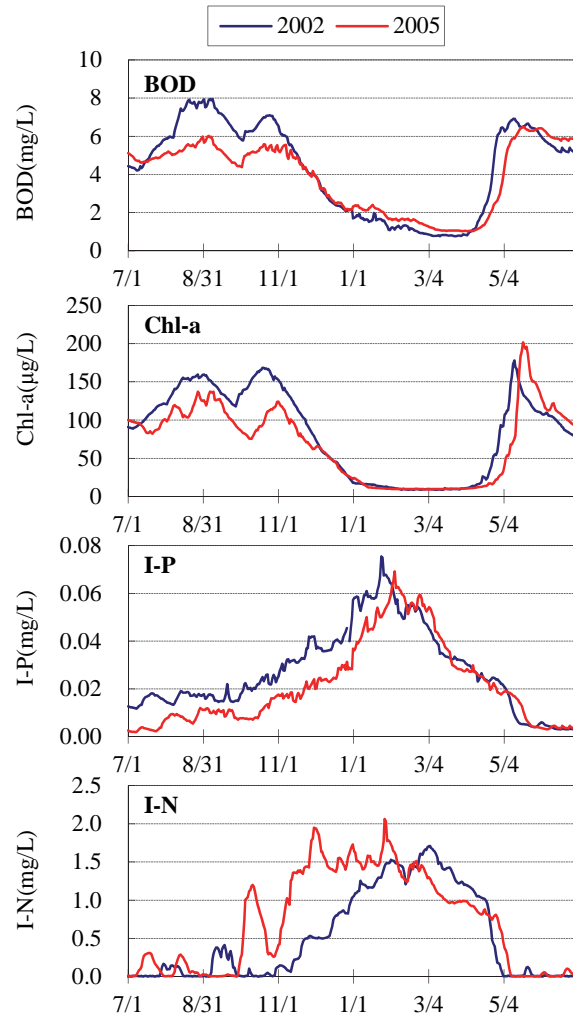


Fig.30 Comparison of calculated value between warm year and cold year.

increasing.

(5) The reduction in the duration of ice cover does not have major effects on water quality deterioration after the breakup of ice, and the water quality after the thawing period varies depending on the air temperature.

(6) The simulation model developed by taking ice cover into account is capable of reproducing spatio-temporal phenomena.

(7) The simulation model can be used for evaluating processes that take place between the freeze-over date and the breakup date, despite the lack of observation data for the thawing period.

In the Barato River, the BOD increases in April and May due to the growth of diatoms, and water is channeled from other rivers from June onward in order to mitigate plankton growth during summer. Increasingly complex factors, such as recent climate changes and unusual natural phenomena, affect the quality of river water. In light of this, the authors of this paper will utilize the simulation model for the following purposes:

1. Estimating the effects of climate change on

water quality by using an appropriate climate change scenario.

2. Proposing farsighted strategies for water quality improvement on the basis of an accurate understanding of the current situations.

ACKNOWLEDGMENT: This paper is based on the Barato River Environmental Survey that was conducted for Stream Renaissance II (an immediate action program for water environment improvement) by the Sapporo Development and Construction Department of the Hokkaido Regional Development Bureau. The authors are grateful to the Sapporo Development and Construction Department for the valuable data that were made available for this paper.

REFERENCES

- 1) Solomon, S., Qin, D., Manning, M., Chen, Z., Marquis, M., Averyt, K. B., Tignor, M. and Miller, H. L. : Contribution of Working Group I to the Fourth Assessment Report of the Intergovernmental Panel on Climate Change, 2007, Cambridge University Press, Cambridge, United Kingdom and New York, NY, USA, 2007.
- 2) Fukushima, T., Kaminishi, H., Matsushige, K., and Harasawa, H. : Influence of meteorological conditions on the water quality of a shallow eutrophic lake, *J. Japan Society on Water Environment*, Vol.21, No.3, pp.180-187, 1998.
- 3) Fukushima, T., Ozaki, N., Kawashima, K., Harasawa, H., and Kojiri, T. : Statistical analysis on the influences of climate changes on river and lake water quality, *Annals of Disas. Prev. Res. Inst. Kyoto Univ.*, No.43, B-2, pp.97-107, 2000.
- 4) Mori, K. : Changes in hydrological environment from the viewpoint of global warming., *Journal of Geography*, No.116(1), pp.52-61, 2007.
- 5) Yanagi, T. : The chemical and biological consequences of mechanisms of its generation, maintenance, variability and disappearance, *Oceanography in Japan*, Vol. 13, No. 5, pp. 451-460, 2004.
- 6) Michioku, K., Kanda, T. and Ishikawa, Y. : Behaviors of contaminated hypolimnetic water with inverse temperature gradient and its effect on reservoir eutrophication, *Journal of Japan Society of Civil Engineers*, No. 740/II-64, pp. 45-62, 2003.
- 7) Yoshikawa, K. and Okubo, K. : Convective transport of dissolved oxygen into the hypolimnion of deep lakes, *Journal of Japan Society of Civil Engineers B*, Vol. 64, No. 1, pp. 41-48, 2008.
- 8) Chikita, K., Fukuyama, R., Sakamoto, H. and Nakamichi, K. : Dynamic behaviours of 'dead water' in a coastal lagoon, Lake Harutori, Kushiro, Hokkaido: Field measurements for the ice-covered period, *Geophysical Bulletin of Hokkaido University*, No. 60, pp. 13-28, 1997.
- 9) Nakamura, Y., Aoi, T. and Kurogi, M. : The seasonal change of phytoplankton in Lake Abashiri, *Journal of the Graduate School of Environmental Science, Hokkaido University*, Vol. 3, No. 1, pp. 35-46, 1980.
- 10) Ohtaka, A., Kamiyama, T., Nagao, F., Kudo, T., Ogasawara, T. and Inoue, E. : Mixing pattern and bathymetric distribution of zoobenthos in an interconnected lake system in the Tsugaru-Juniko Lakes, Aomori Prefecture, northern Japan, *Japanese Journal of Limnology*, Vol. 71, pp. 113-128, 2010.
- 11) Cooke, G. D. and Kennedy, R. L. : Eutrophication of northeastern Ohio lakes, *The Ohio Journal of Science*, Vol. 150, No. 70 (3), 1970.
- 12) Priscu, J. C., Downes, M. T. and McKay, C. P. : Extreme supersaturation of nitrous oxide in a poorly ventilated Antarctic lake, *Limnol. Oceanogr.*, No. 41 (7), pp. 1544-1551, 1996.
- 13) Veillette, J., Martineau, M. J., Antoniadis, D., Sarrazin, D. and Vincent, W. F. : Effects of loss of perennial lake ice on mixing and phytoplankton dynamics: Insights from High Arctic Canada, *Annals of Glaciology*, No. 51 (56), pp. 56-70, 2010.
- 14) Hamahara, Y., Kato, K. and Nakatsugawa, M. : Comprehensive analysis of eutrophication in the Barato River, calculation of water balance, heat balance and flow, *Monthly Report, Civil Engineering Research Institute of Hokkaido*, No. 613, pp. 3-15, 2004.
- 15) Sugihara, K., Hamahara, Y., Kato, K. and Nakatsugawa, M. : Comprehensive analysis of eutrophication in the Barato River—Estimation of load balance and simulation of water quality using ecosystem model—, *Monthly Report, Civil Engineering Research Institute of Hokkaido*, No. 615, pp. 10-24, 2004.
- 16) Hokkaido Regional Development Bureau : Water Quality Observation Duties Report of Ishikari River in 2011, 2011.
- 17) Horne, A. J. and Goldman, C. R. : *Limnology*, McGraw-Hill, New York, 1994.
- 18) The Public Works Research Institute, Ministry of Construction: The numerical model of cold turbid water and eutrophication in dam reservoir (No. 2), *Technical Note of PWRI*, No. 2443, 1987.
- 19) Matsuo, N. : Problems related to hydrology of the lake environment, *Summer Workshop Lecture Practices for Water Engineering*, A-7, pp. 1-20, 1989.
- 20) Matsuo, N., Yamada, M. and Somiya, I. : Relation between the hydrodynamic characteristics of stratified flows and freshwater red-tide near the upstream end of a reservoir, *Annual Journal of Hydraulic Engineering, JSCE*, Vol. 40, pp. 575-581, 1996.
- 21) Morikita, Y. and Amano, K. : The study on the prediction and assessment model of dam reservoir water quality, *Research Report of PWRI*, No. 182, pp. 1-109, 1996.
- 22) Kondo, J. : *Meteorology of Water Environment*, Asakura Publishing, 1994.
- 23) Yoshikawa, Y., Watanabe, Y. and Hirai, Y. : Consideration of an ice-sheet conformation factor in the ice-covered river, *Proceeding of Hokkaido Chapter of JSCE*, Vol. 65, B-2, 2008.
- 24) Sugihara, K., Nakatsugawa, M. and Seiji, M. : Evaluation of hydrologic cycle restoration based on water environment of waters flowing from urban area, *Annual Journal of Hydraulic Engineering, JSCE*, Vol. 53, pp. 1111-1116, 2009.
- 25) Sugihara, K., Nakatsugawa, M. and Seiji, M. : Influence of climatic change on water quality of stagnated waters that freeze over, *Annual Journal of Hydraulic Engineering, JSCE*, Vol. 54, pp. 1525-1530, 2010.

(Received October 19, 2015)